

SUBSTELLAR



Funded by
the European Union

The Euclid Mission in the context of the Gaia NIR mission

Eduardo L. Martín(IAC)

PI Substellar ERC Advanced grant

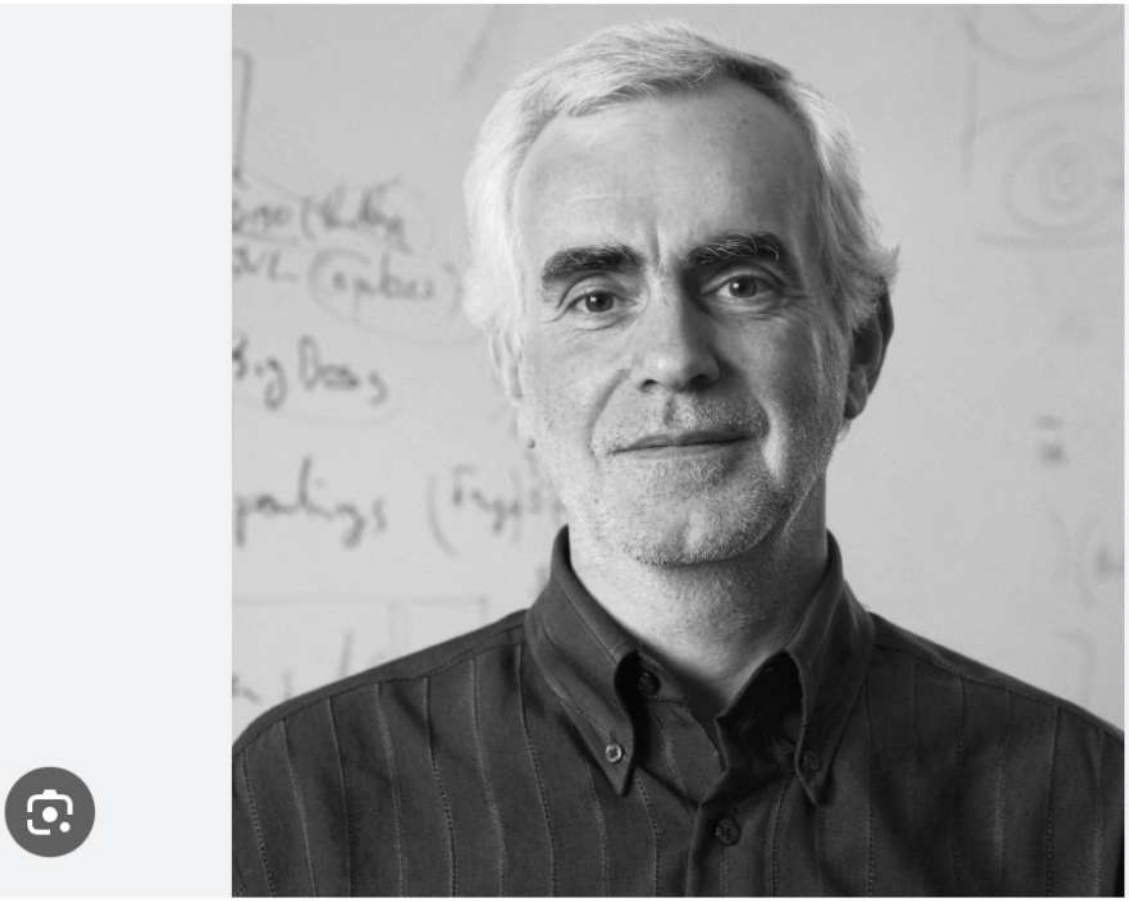
ESA Indepent Legacy Scientist in the Euclid Science Team

ESA appointed scientist in the Nancy Grace Roman space mission





Euclid Consortium





Yannick Mellier, 1958–2025 – Euclid Consortium

Creador: Jean Mouette

A&A, 697, A1 (2025)
https://doi.org/10.1051/0004-6361/202450810
© The Authors 2025

94 pages
1136 authors
Cited: 655

Astronomy & Astrophysics

Special issue

Euclid on Sky

Euclid

I. Overview of the *Euclid* mission★

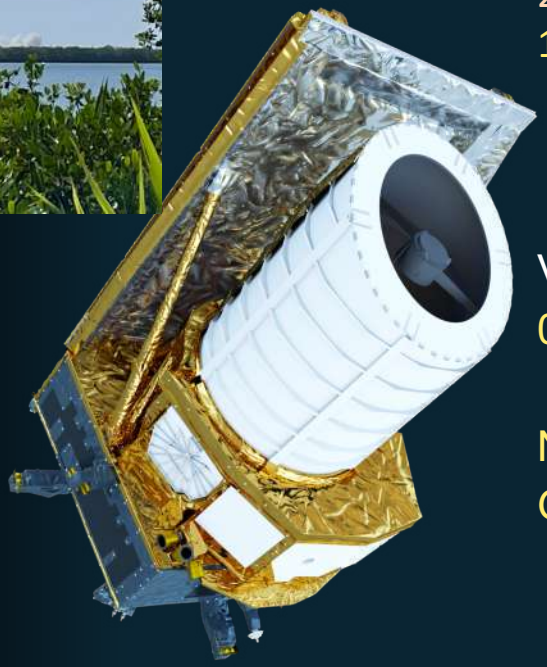
Euclid Collaboration: Y. Mellier[1,2,★★], Abdurro'uf[3], J. A. Acevedo Barroso[4], A. Achúcarro[5,6], J. Adamek[7], R. Adam[8], G. E. Addison[3], N. Aghanim[9], M. Aguena[10], V. Ajani[11,12,13], Y. Akrami[14,15], A. Al-Bahlawan[16], A. Alavi[17], I. S. Albuquerque[18], G. Alestas[14], G. Alguero[19], A. Allaoui[20], S. W. Allen[21,22,23], V. Allevato[24], A. V. Alonso-Tetilla[25], B. Altieri[26], A. Alvarez-Candal[27,28], S. Alvi[29], A. Amara[30], L. Amendola[31], J. Amiaux[11], I. T. Andika[32,33], S. Andreon[34], A. Andrews[35], G. Angora[24,29], R. E. Angulo[36,37], F. Annibali[35], A. Anselmi[38], S. Anselmi[39,40,41], S. Arcari[29,42], M. Archidiacono[43,44], G. Aricò[7], M. Arnaud[45,46], S. Arnouts[20], M. Asgari[47], J. Asorey[48], L. Atayde[18], H. Atek[2], F. Atrio-Barandela[49], M. Aubert[50,51], E. Aubourg[10,45], T. Auphan[52], N. Auricchio[35], B. Aussel[53], H. Aussel[11], P. P. Avelino[54,55], A. Avgoustidis[56], S. Avila[57], S. Awan[16], R. Azzollini[16], C. Baccigalupi[58,59,60,61], E. Bachelet[62], D. Bacon[63], M. Baes[64], M. B. Bagley[65], B. Bahr-Kalus[51,66], A. Balaguera-Antolinez[67,68], E. Balbinot[69,70], M. Balcells[67,68,71], M. Baldi[72,35,73], I. Baldry[74], A. Balestra[75], M. Ballardini[29,35,42], O. Ballester[57], M. Balogh[76,77], E. Bañados[78], R. Barbier[51], S. Bardelli[35], M. Baron[51], T. Barreiro[18,79], R. Barrena[80], J.-C. Barriere[81],



EUCLID

ESA-led

2,1 t
1.2 m



VIS
0.55 - 0.9 μm

NISP
GRISM 1.25 - 1.85 μm
Y, J, H

Launched from Cabo Cañaveral by Space X

1 July 2023



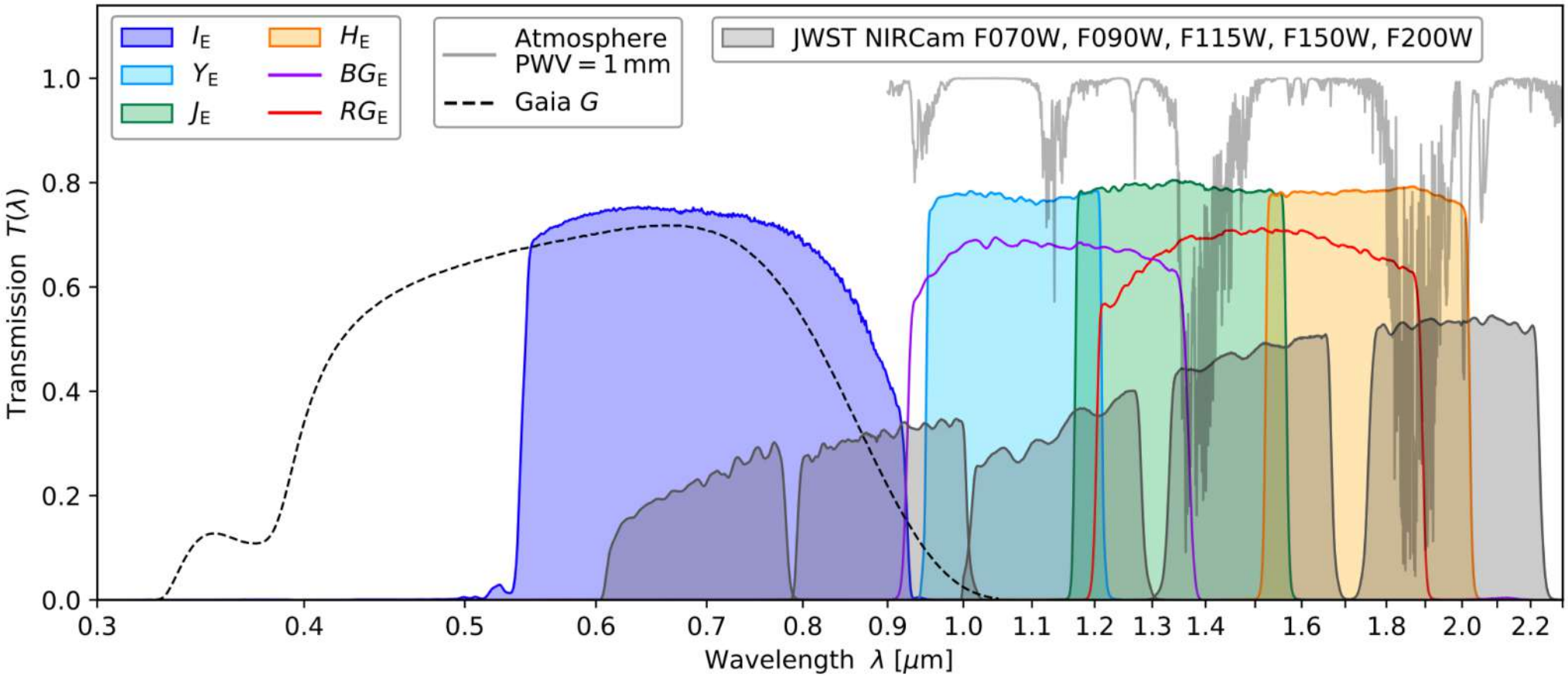


Fig. 11. Spectral response of *Euclid*'s imaging (VIS: I_E; NISP: Y_E, J_E, H_E) and spectroscopic channels (NISP: BG_E, RG_E) at the beginning of the mission. The expected transmission loss at the end of the mission due to space weathering and non-volatile contamination is at most 0.05. For reference we show the *Gaia G* passband from their third data release (Gaia Collaboration 2023b), the atmospheric transmission for a precipitable water vapour level of 1.0 mm (Rothman et al. 2013), and some of the JWST passbands of their Near Infrared Camera (NIRCam; Rieke et al. 2005).

Euclid provides unprecedented depth over Large área with High spatial Resolution

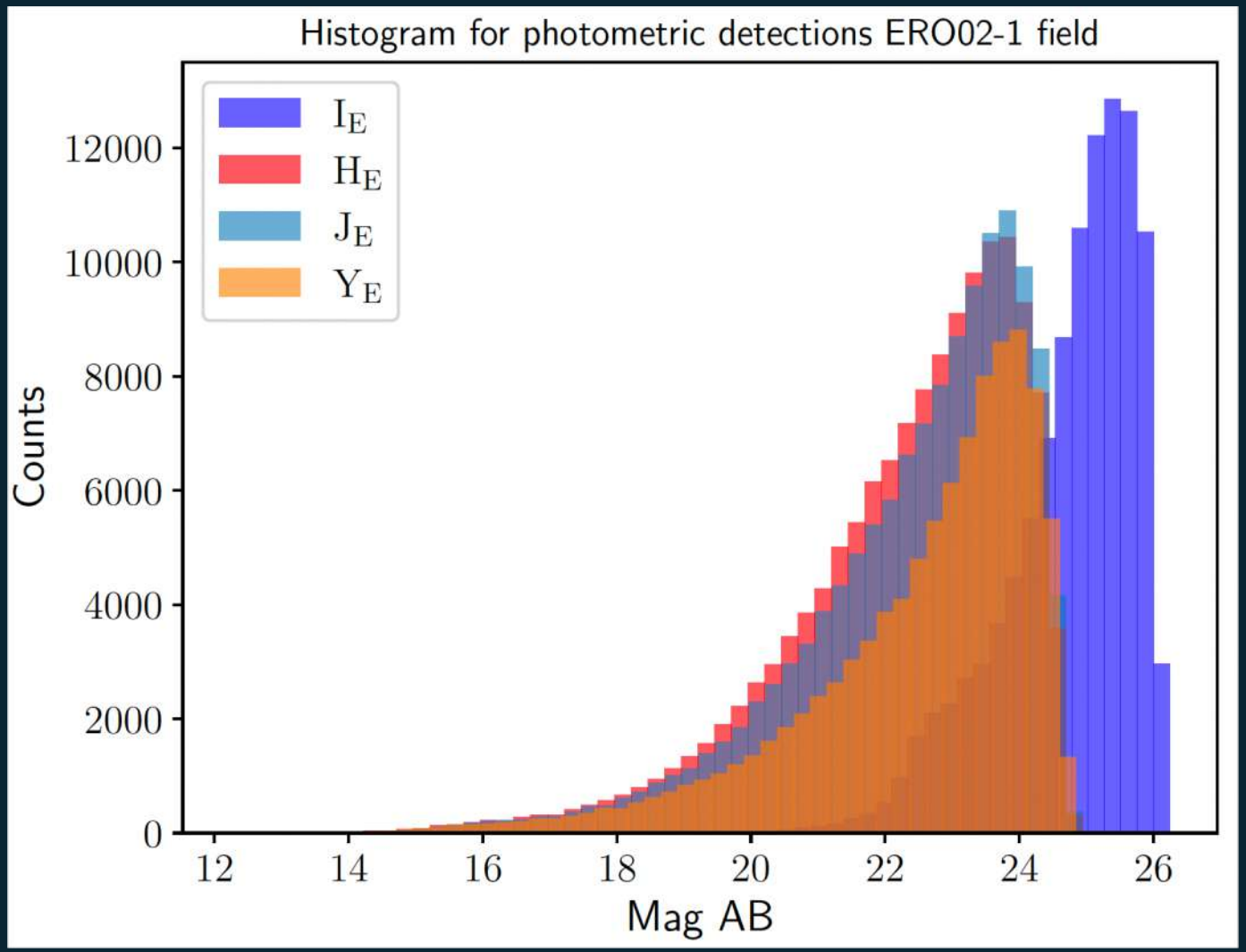


Table 2. General median properties of the 17 *Euclid* ERO fields with a 0.60 deg^2 sky coverage for single ROS observations.

Band	I_E	Y_E	J_E	H_E	Unit/note
FWHM	0.157	0.477	0.486	0.492	arcsec
FWHM	1.57	1.59	1.62	1.64	pixel
Pixel sampling	0.1	0.3	0.3	0.3	arcsec pixel^{-1}
Depth 5 σ stars	27.12	*24.45*	*24.60*	*24.52*	mag (PSF or *aperture* photometry)
Depth 10 σ galaxies	25.29	22.97	23.22	23.31	mag (Kron magnitude)
Limiting surface brightness	29.9	28.2	28.4	28.4	mag arcsec^{-2}, $10'' \times 10''$ scale at 1 σ
Sky background	22.3	22.1	22.2	22.3	mag arcsec^{-2}, range: [–0.5, +0.5]
Photometric zero point	30.13	30.0	30.0	30.0	mag, ADU (first ERO public data release)
Astrometry (internal)	5.1	14.9	14.9	14.9	mas
Saturation	20 900	141 000	107 000	111 000	ADU
Total number of sources	11 359 274	5 257 808	5 257 808	5 257 808	All ERO (common detection on NISP)

Notes. Tables B.1 and B.2 list all properties per ERO field. All magnitudes are instrumental and in the AB system. The range of the sky background reflects the ecliptic latitudes covered across the ERO fields.

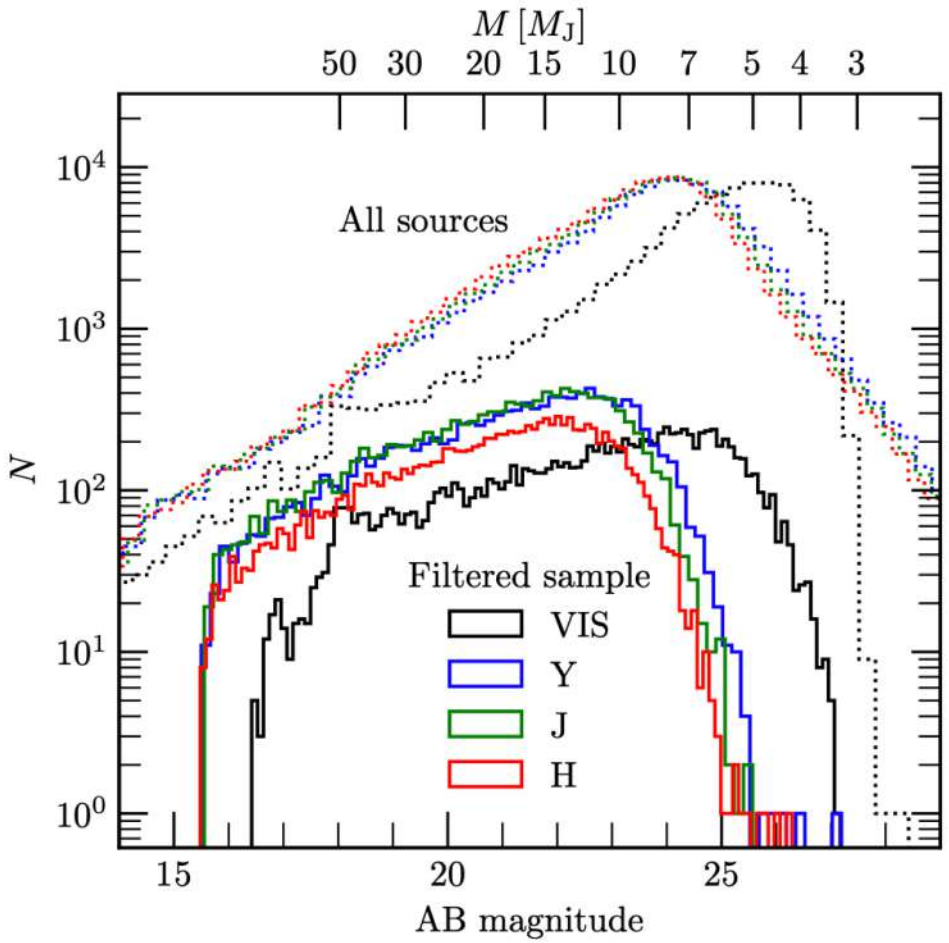


Fig. 9. Number counts of *Euclid* sources in the catalogue of the σ Orionis region before and after filtering. The correspondence between VIS magnitudes and masses has been made using the ATMO 3 Myr isochrone.

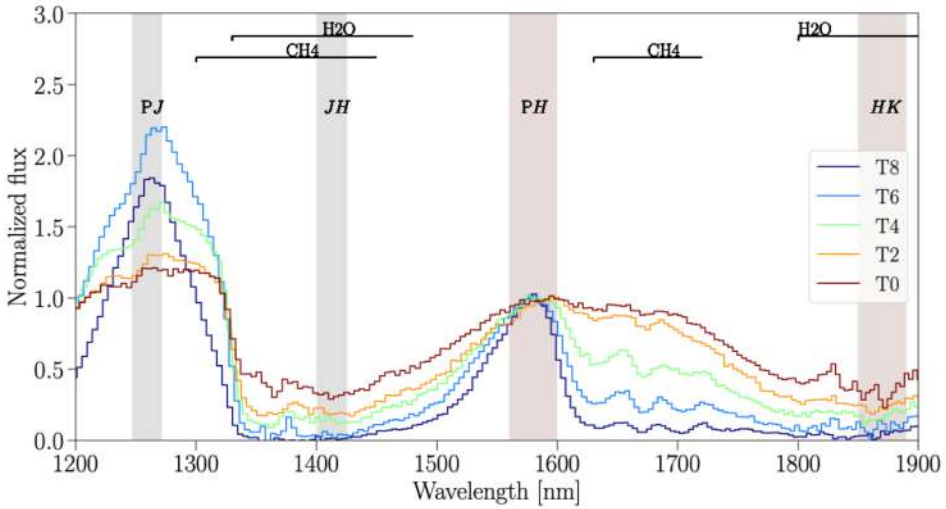


Figure 2. Spectral regions used for the spectral index search, plotted over the spectra of the T dwarf standard templates (references in Appendix A).

spectral range covered by NISP that a fast algorithm computing ratios can easily detect these absorption bands.

Table 1
New Late L and T Dwarfs Found by the Spectral Index Search Algorithm

Alias	SpT	P*J*–*JH*	P*H*–*JH*	P*H*–*HK*
E528241	T5	0.9	0.7	0.7
E265716	T4p	0.9	0.9	0.9
E523574	T4	0.9	0.8	0.8
E273062	T3p	0.9	0.8	0.6
E536416	T2:	0.8	0.8	0.8
E273015	T1:	0.8	0.8	0.8
E644720	T1:	0.7	0.6	0.6
E511520	T1:	0.8	0.8	0.9
E267056	L9:	0.7	0.7	0.5
E517518	L9	0.6	0.6	0.5
E271934	L9p	0.7	0.6	0.4

Note. The third to fifth columns are the search indices defined in the text. The SpT is described in Section 3.3.

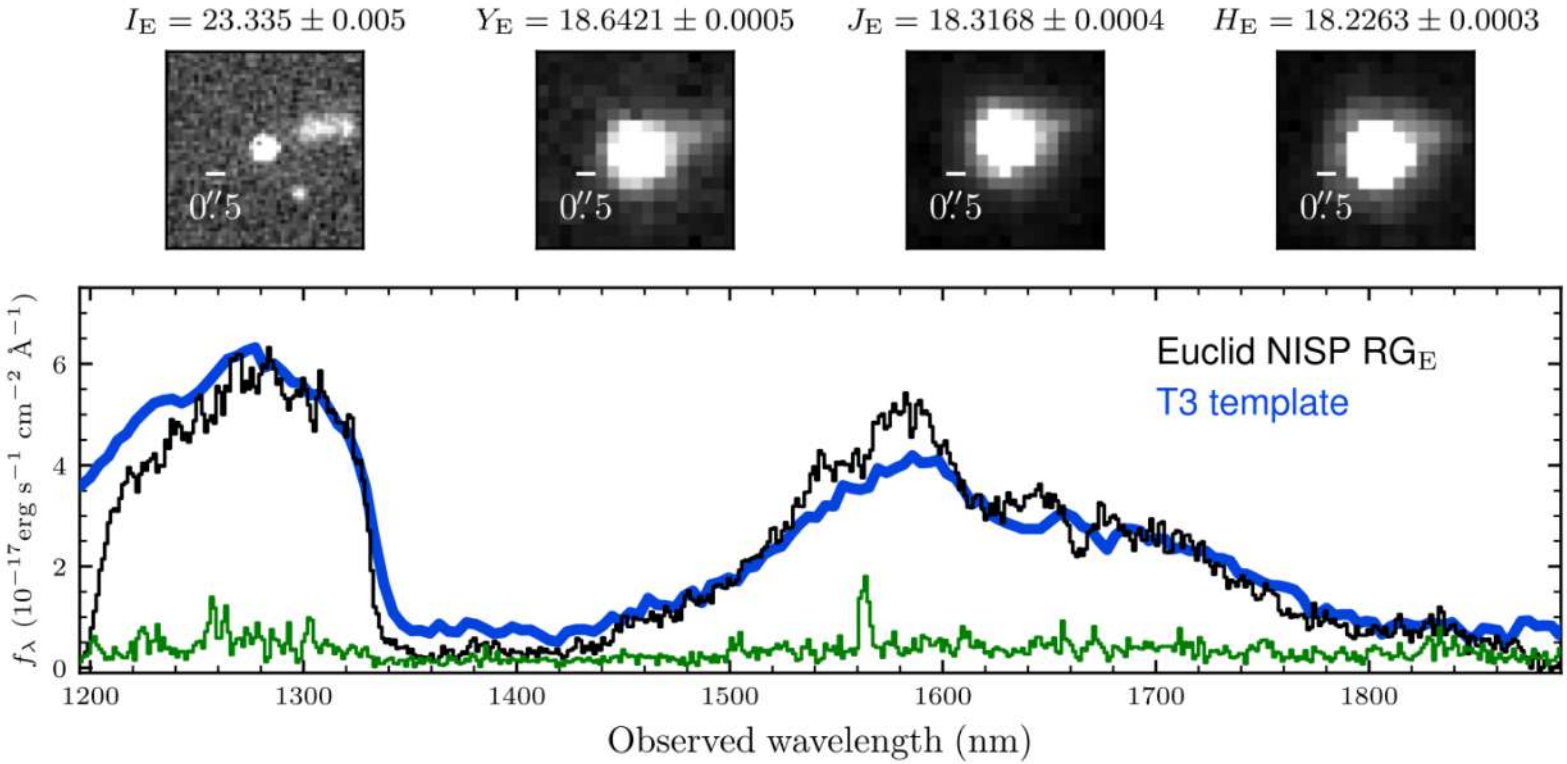


Figure 3. *Top:* Postage stamps of the T3 dwarf EUCL J002516.31−491618.5. The *Euclid* I_E, Y_E, J_E, and H_E images are 5 *arcsec* on a side. *Bottom:* NISP RG$_E$ grism spectrum (black line and the uncertainties in green). The blue line shows a template of a T3 binary: 2MASS J12095613−1004008 (Burgasser et al. 2004; Dupuy & Liu 2012).

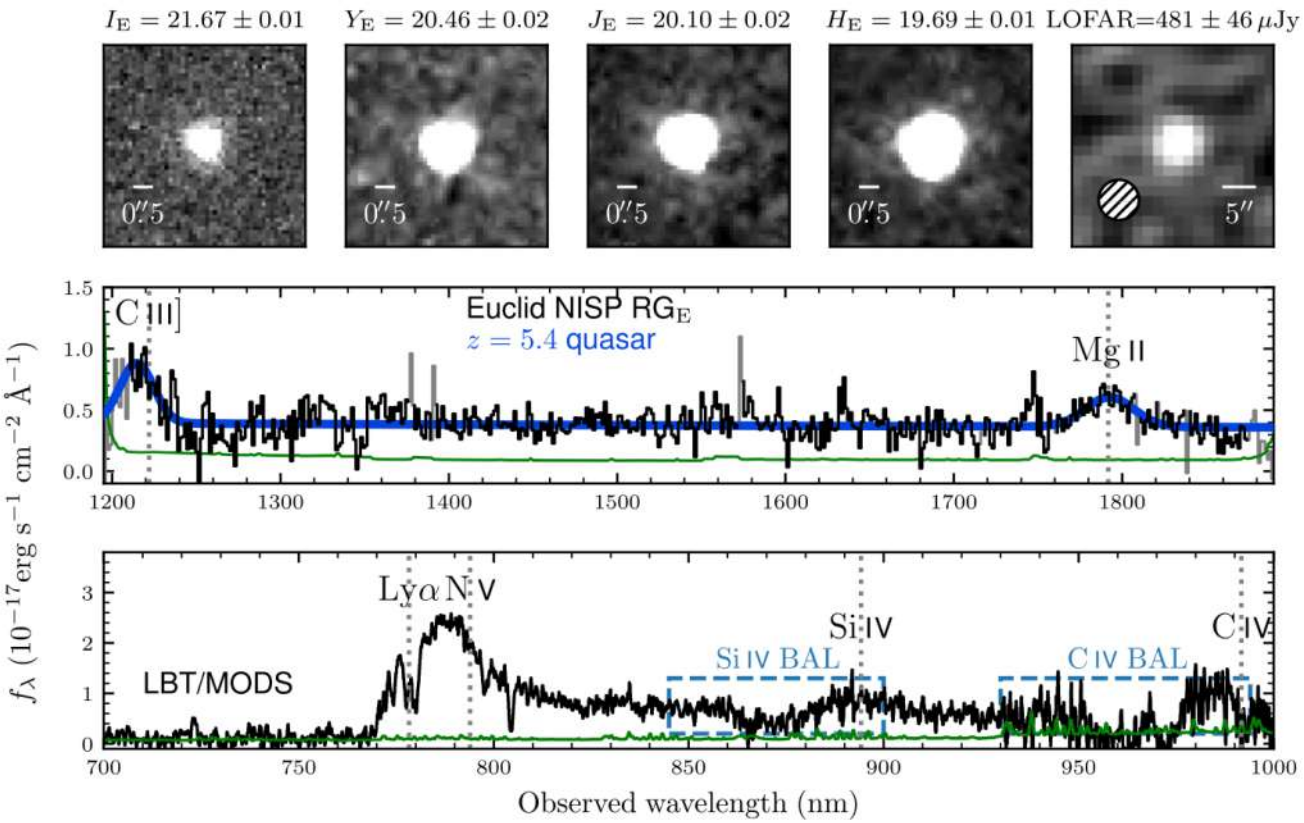
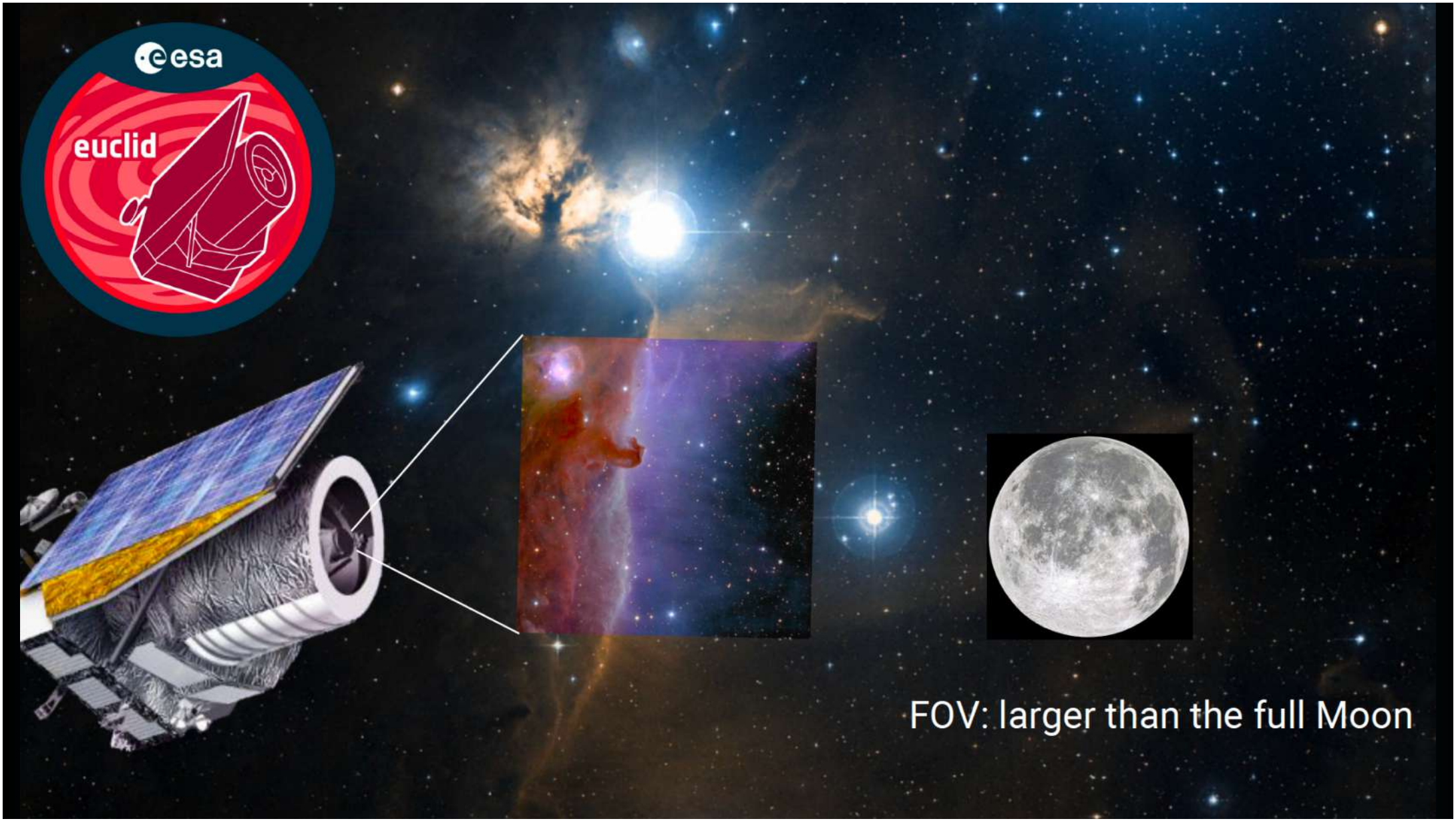


Figure 5. *Top:* Postage stamps of the $z = 5.4$ quasar EUCL J181530.01+652054.0. The *Euclid* I_E, Y_E, J_E, and H_E images are 5″ on a side while the LOFAR image is 30″ on a side. The LOFAR beam is shown on the lower left of its panel. *Middle:* NISP grism RG_E spectrum (black line; masked pixels are in grey, and the uncertainties in green). The blue line shows the best-fitting power-law emission plus C III] and Mg II broad emission lines, identifying this as a quasar at $z_{Mg\,II} = 5.404 \pm 0.007$. *Bottom:* LBT/MODS optical spectrum (black line and uncertainties in green), confirming the quasar nature of EUCL J181530.01+652054.0. The vertical dashed lines correspond to the expected position of the labelled emission lines based on the Mg II redshift. The dashed rectangles indicate the Si IV and C IV BAL regions shown in Fig. 7.


esa
euclid
FOV: larger than the full Moon

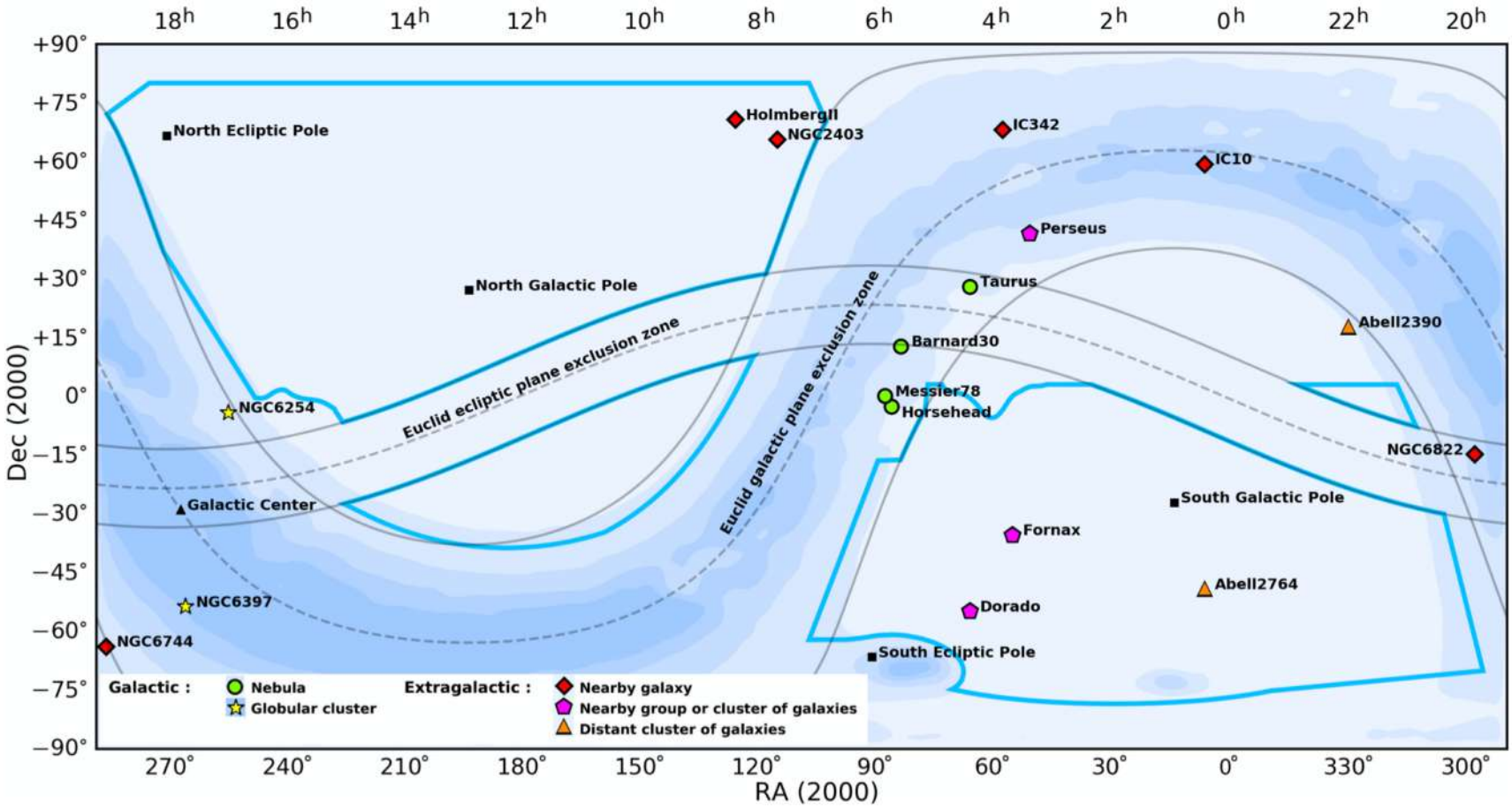


Fig. 1. Location, name, and nature of the 17 ERO fields on an all-sky map. The general RoI of the EWS is highlighted by the four blue contours. These outlines signify that some of the ERO targets will be revisited in the coming years. The distinctive nature of the ERO programme facilitated explorations spanning from the Galactic plane to the southern Galactic cap, areas that were accessible during the observation period. This range of coverage showcases the ERO programme's goal to venture across a wide variety of astronomical phenomena and regions. The blue background depicts the stellar density across the sky.

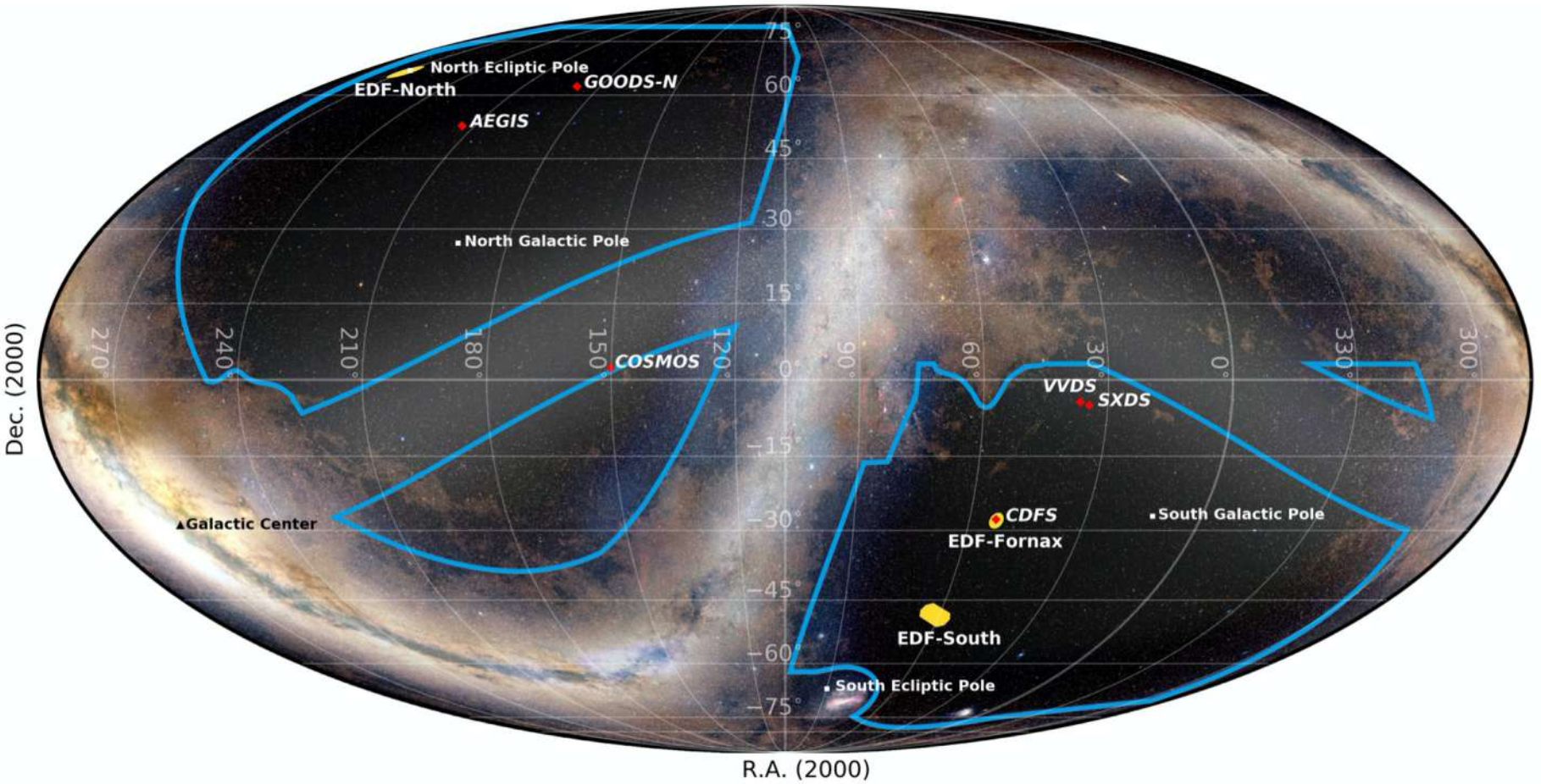
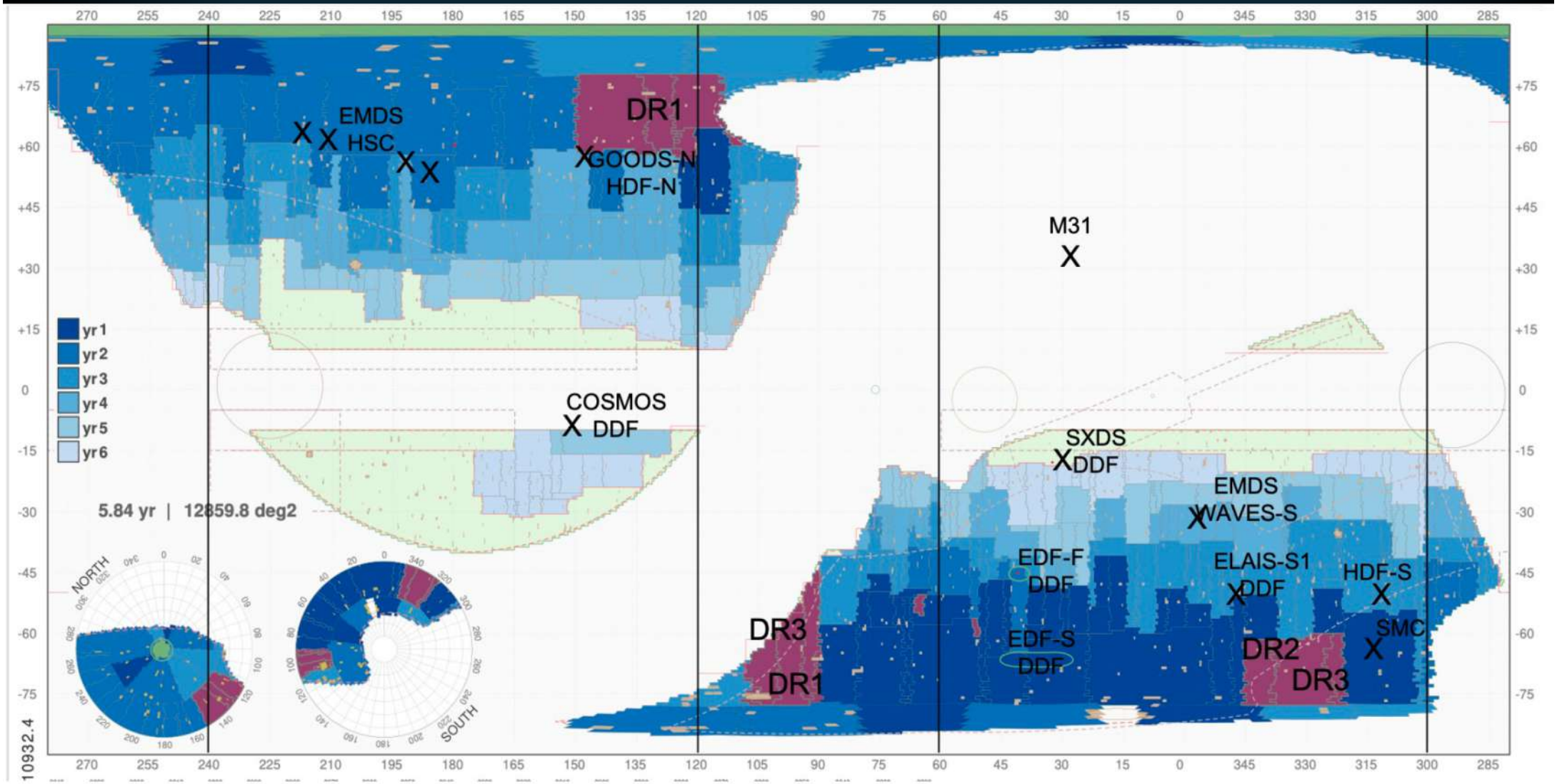


Fig. 14. *Euclid* RoI in an all-sky Mollweide projection. The blue borders enclose the 16 000 deg^2 RoI that contains the observed sky of the Euclid Wide Survey. The RoI excludes the Galactic and ecliptic planes. The triangular southern 'island' near RA = 330° is restricted in size since the LSST does not extend to more northern latitudes. The Euclid Deep Fields are shown in yellow and the auxiliary fields with red marks (not to scale).


EMDS
HSC
DR1
GOODS-N
HDF-N
M31
COSMOS
DDF
SXDS
DDF
EMDS
WAVES-S
EDF-F
DDF
ELAIS-S1
DDF
HDF-S
SMC
EDF-S
DDF
DR3
DR1
DR2
DR3
yr 1
yr 2
yr 3
yr 4
yr 5
yr 6
5.84 yr | 12859.8 deg2
NORTH
SOUTH
10932.4

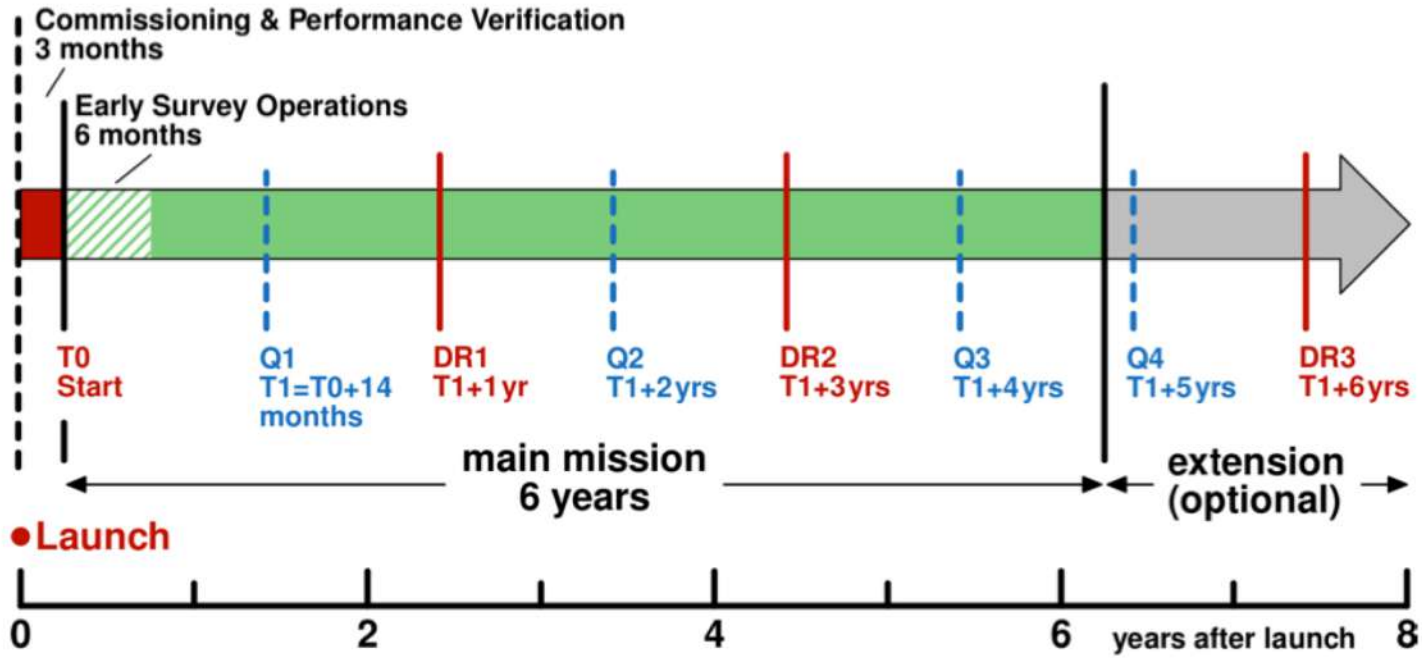


Fig. 35. Tentative timeline for public data releases, indicating the three main DRs as well as four smaller quick releases (Q1–Q4). The moment of release is linked to the start of early survey operations, but unforeseen changes to the mission operation may lead to some changes to this nominal schedule.



IQ1	Q1	IDR1 (no LE3)	IDR1 (no LE3)	IQ2 EGBS	IDR1 (LE3)	IEUDF	Q2 EGBS	DR1	EUDF	IQ3 (TBC)	IDR2	Q3 (TBC)	DR2	IQ4 (TBC)	Q4 (TBC)	IDR3	DR3
Nov 2024	March 2025	Oct 2025	Nov 2025	Feb 25 2026	March 2026	Jun 2026	Jun 24 2026	Oct 22, 2026	May 2027	Jan 2028 TBC	March 2028	May 2028 TBC	March 2029	Jan 2030 TBC	May 2030 TBC	Oct 2030	Oct 2031

Ultracool dwarf science boost!

GAIA

$d_\odot$ = 100 pc (GAIA EDR3, M9)

EWS (EUCLID WIDE SURVEY)

$d_\odot$ = 438 pc (EUCLID WIDE NISP, T0)

$d_\odot$ = 624 pc (EUCLID WIDE NISP, L5)

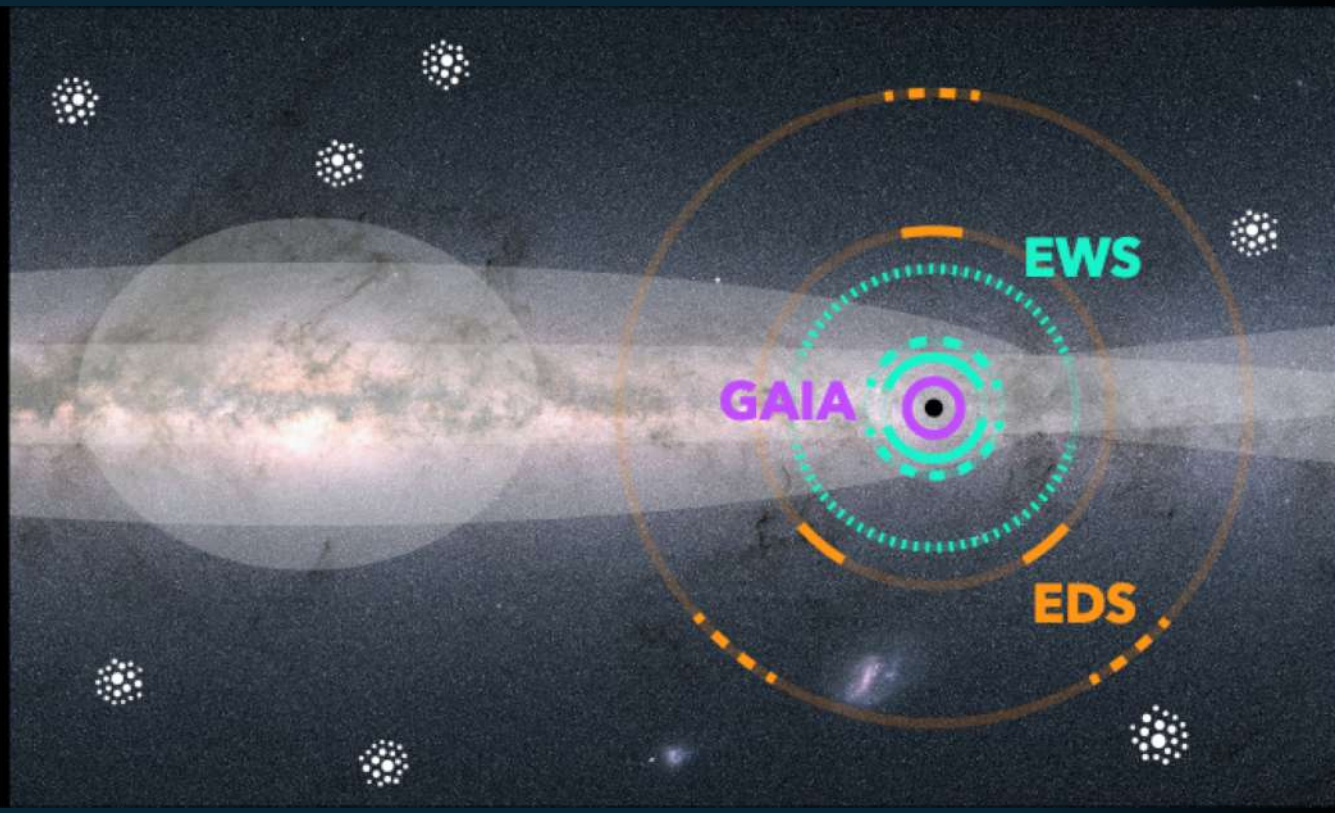
$d_\odot$ = 1751 pc (EUCLID WIDE NISP, M9)

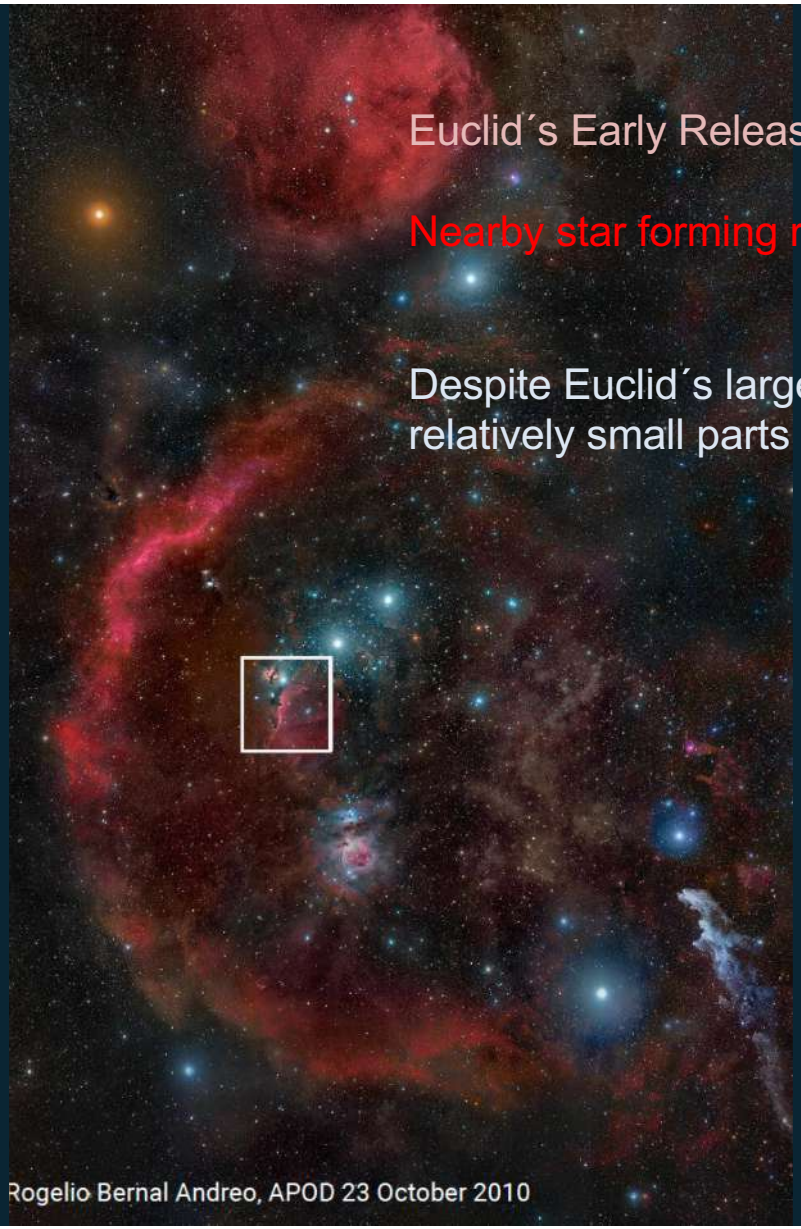
EDS (EUCLID DEEP SURVEY)

$d_\odot$ = 1980 pc (EUCLID DEEP VIS, M9)

$d_\odot$ = 4398 pc (EUCLID DEEP NISP, M9)

HALO-TRACERS





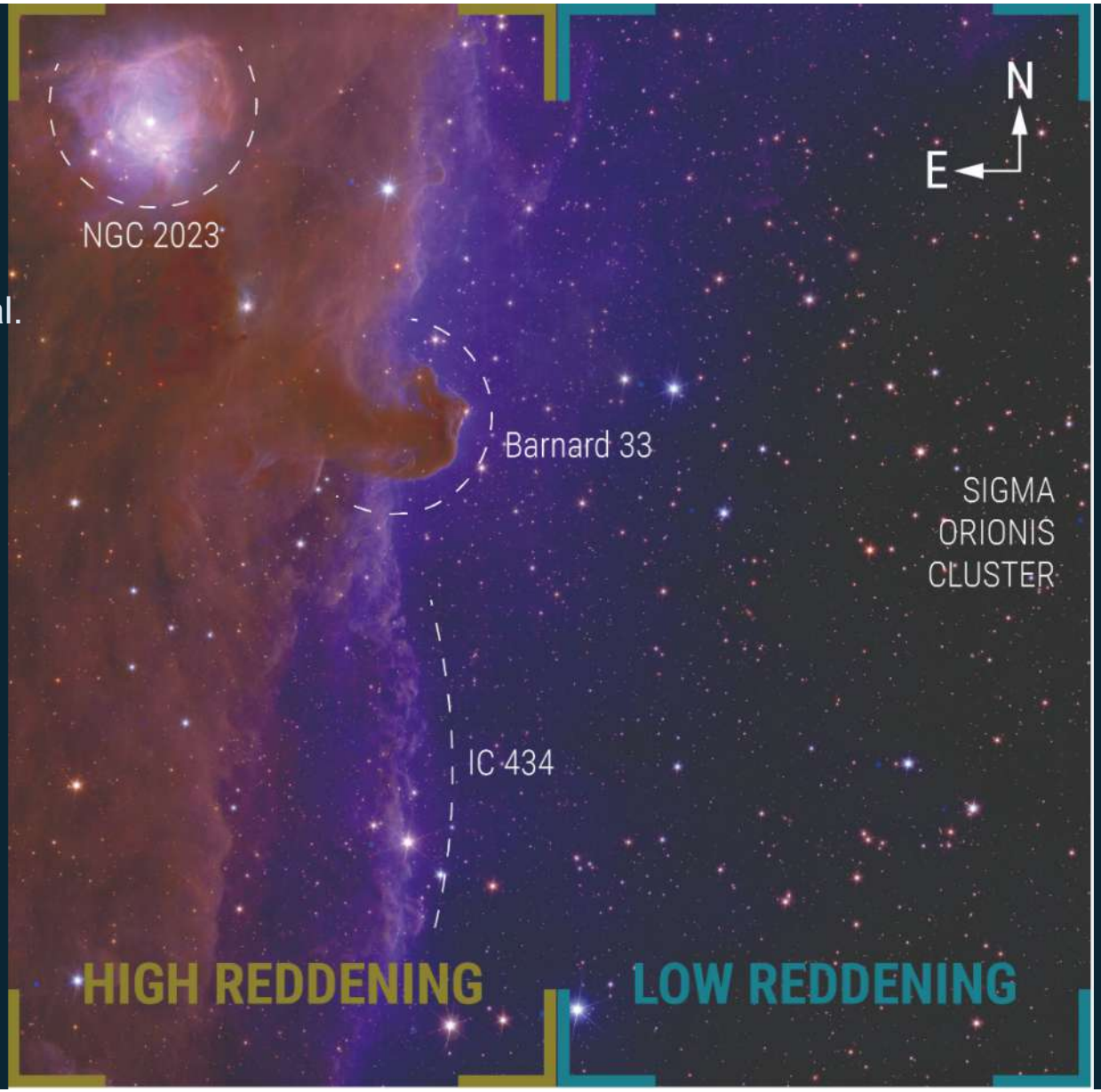
Euclid´s Early Release Observations (ERO)

Nearby star forming regions & very young open clusters

Despite Euclid´s large FoV, ERO program covered relatively small parts of Orion & Taurus SFRs

Euclid on Sky
Special issue
A&A, April 2025

Martín, Zerjal, Bouy et al.



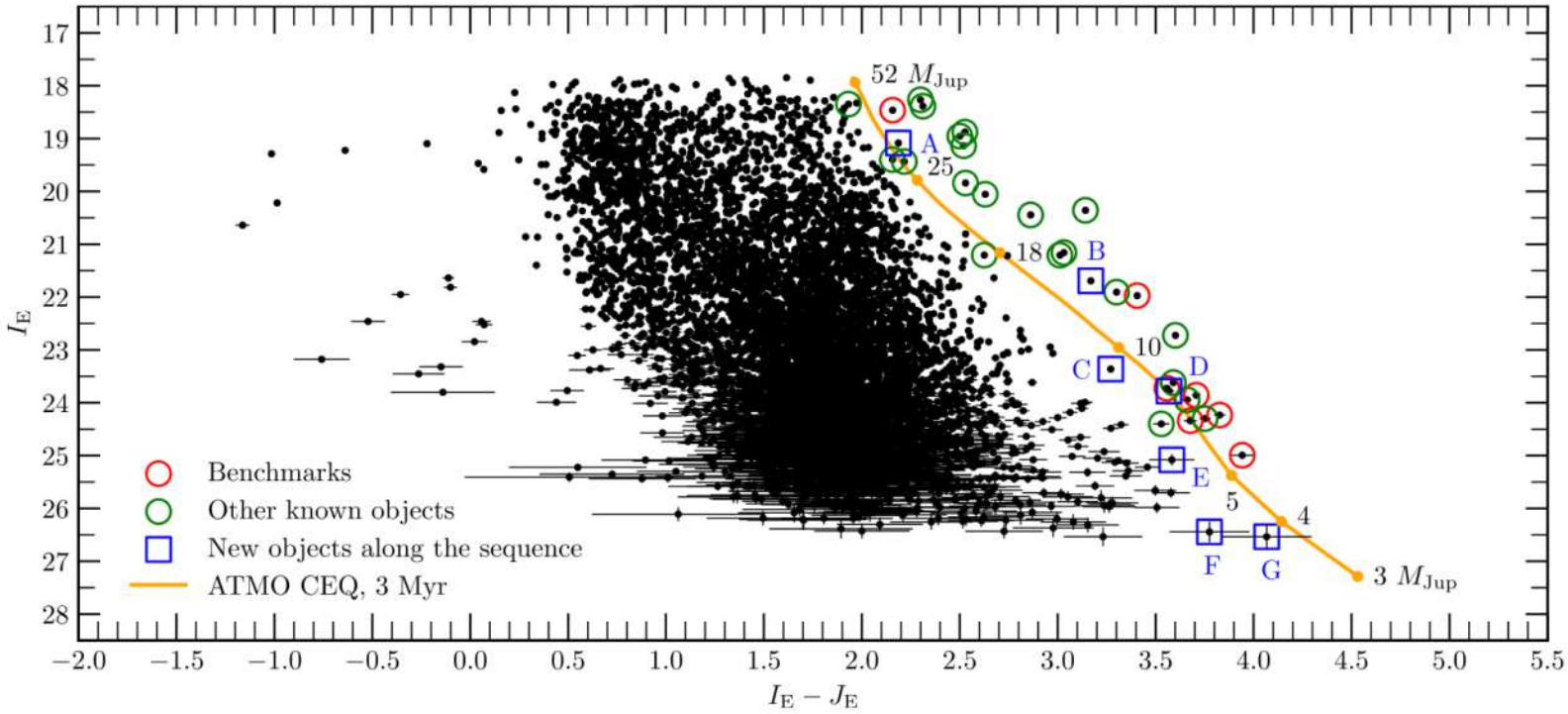
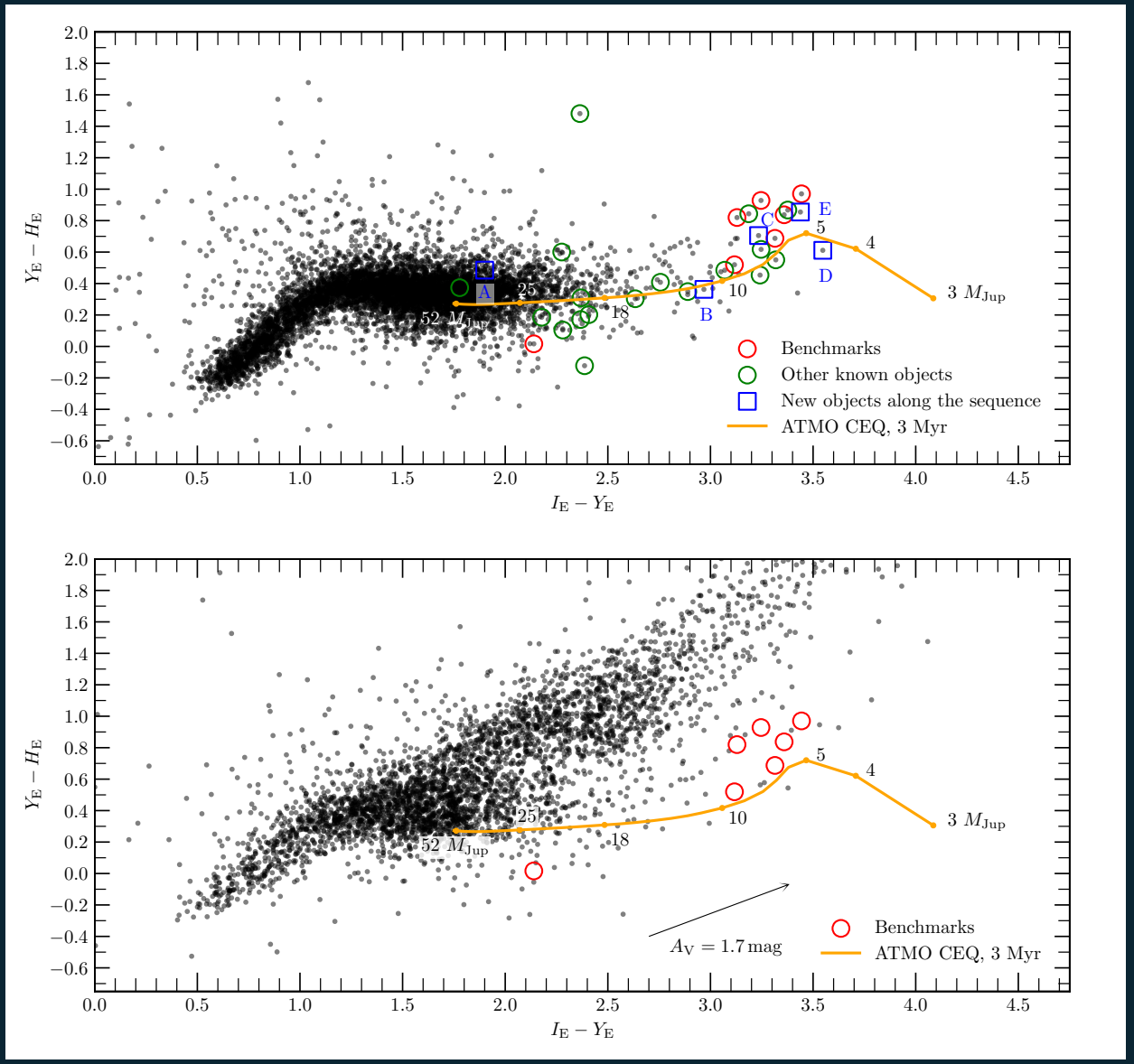
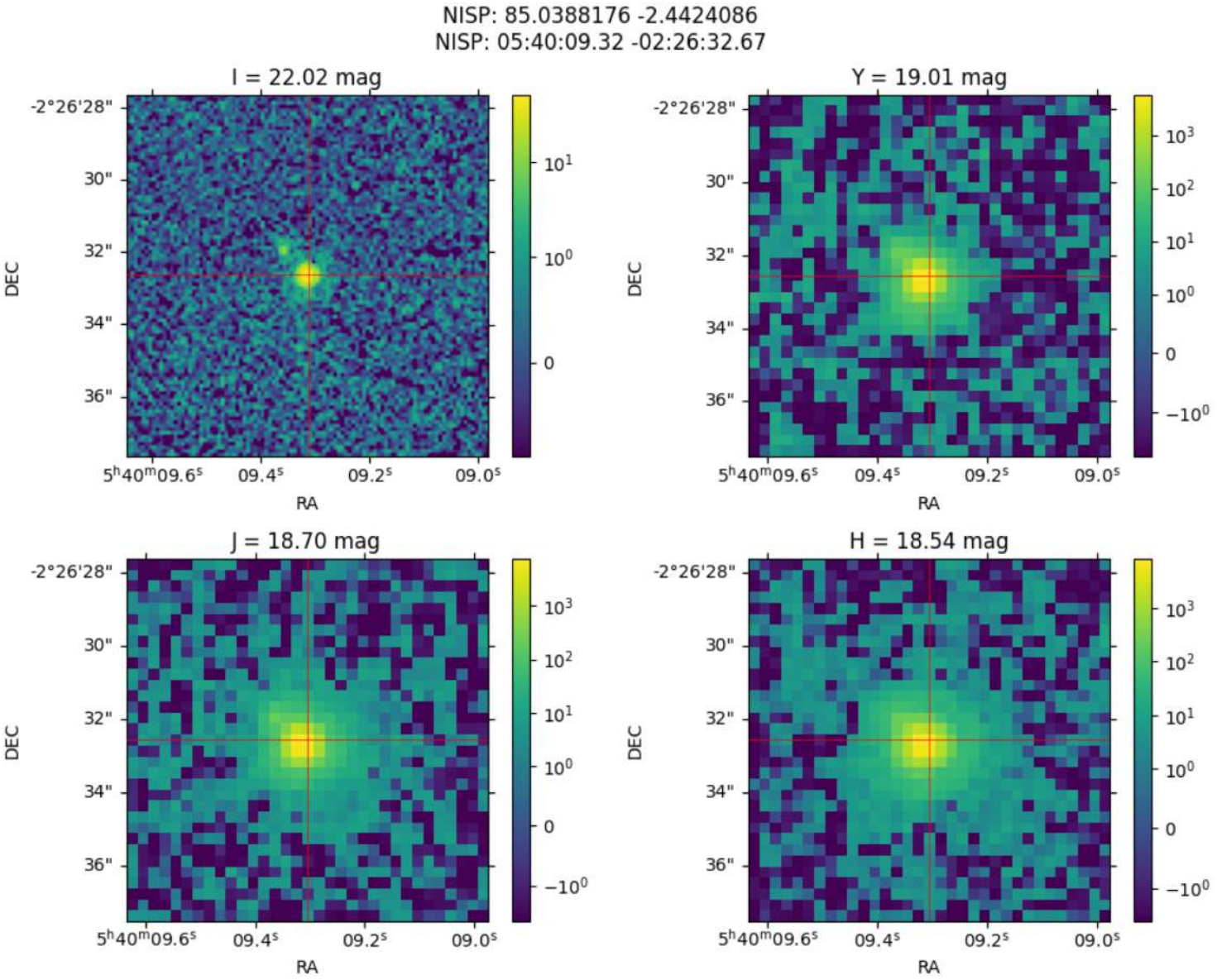


Fig. 4. $I_{\rm E}$ vs. $I_{\rm E} - J_{\rm E}$ colour–magnitude diagram for the σ Orionis part of the FoV. The black points are all the *Euclid* sources that remain after applying all the cuts. Benchmark objects are denoted with red circles. New objects near the cluster sequence are denoted with blue squares and labelled with capital letters. Known sources other than the benchmarks in the σ Orionis cluster are denoted with green circles. An ATMO CEQ isochrone (see Phillips et al. 2020) for an age of 3 Myr and a distance of 402.74 pc is shown. Theoretical masses are labelled on the isochrone.

Euclid color-color diagrams get complex with variable reddening



Euclid resolves wide companions around Rogue Worlds



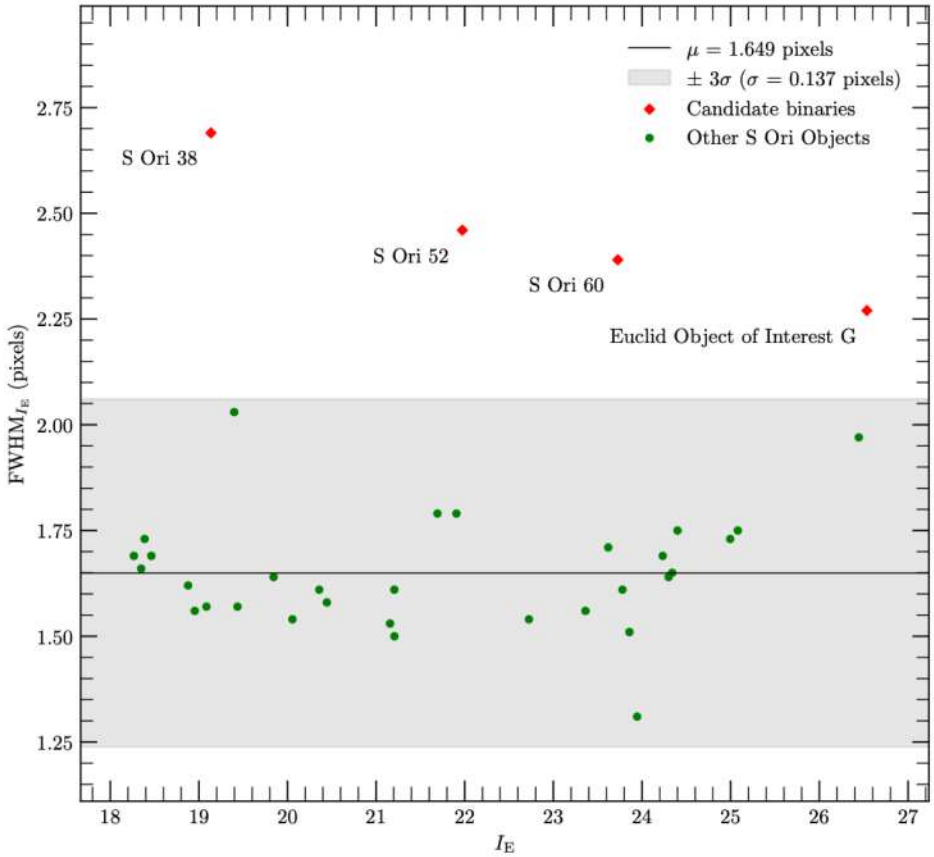


Fig. B.2. *Euclid* VIS FWHM (in pixels) versus I_E apparent magnitude for objects confirmed by *Euclid* to be in the σ Orionis cluster sequence. Both the FWHM and I_E photometry values come from the ERO catalogue. Four objects were found to have FWHM values larger than the mean value of cluster members (more than $3\,\sigma$ significance) and hence are considered as possible binaries that deserve further scrutiny. Two of them are benchmark objects, namely (S Ori 52 and S Ori 60), one is a known object (S Ori 38), and the faintest one is a new discovery (*Euclid* object of interest G).

Gaia & Euclid
complement
each other in
Orion:
Gaia covers stellar IMF
Euclid covers substellar

Little overlap

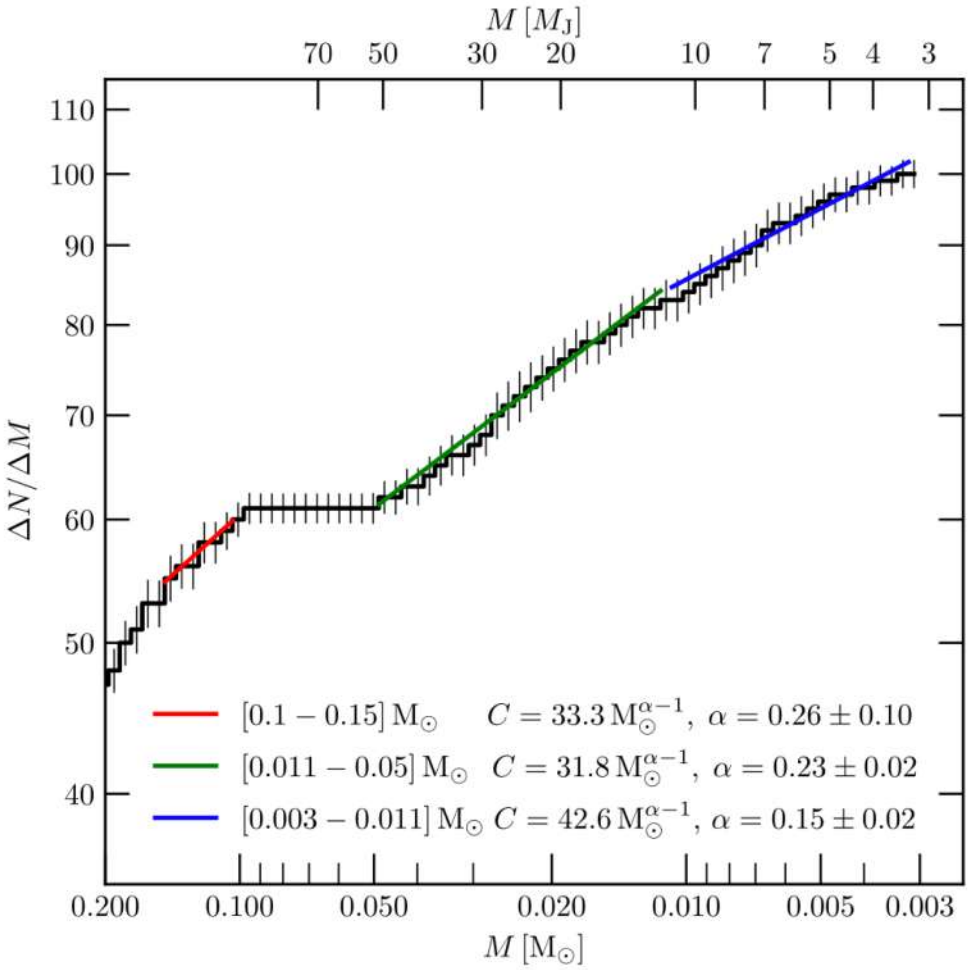


Fig. B.3. Unresolved binary-corrected very low mass *Euclid-Gaia* IMF of the σ Orionis cluster with linear fits in three different mass regions. A 20% unresolved binary frequency of equal mass binaries has been assumed in the simulations.

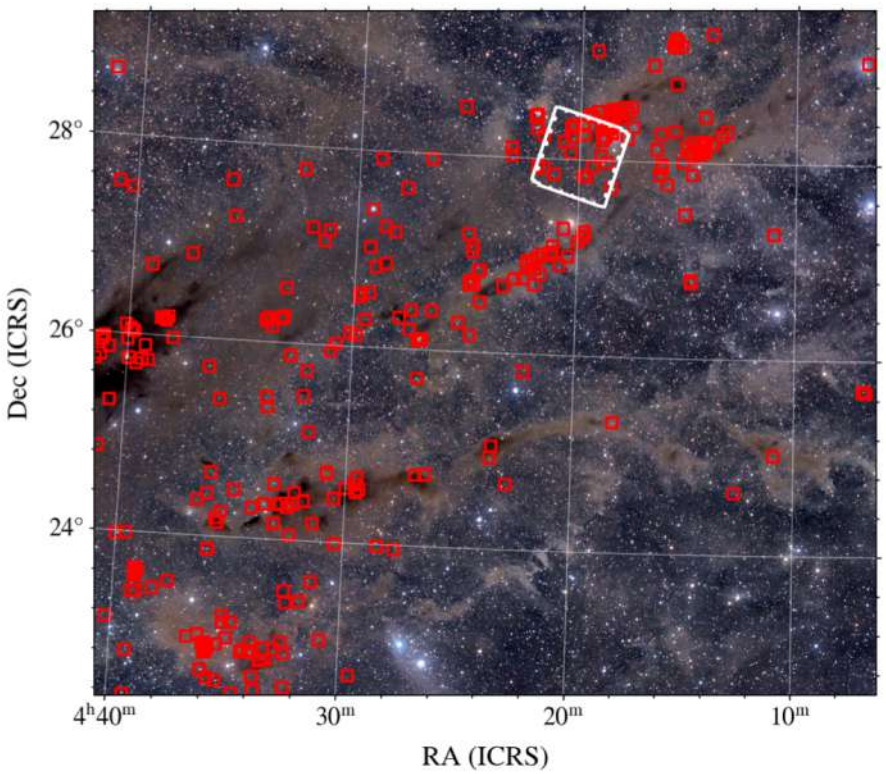


Fig. 1. Photograph of the LDN1495 region showing the Taurus molecular clouds and the Taurus members presented by Galli et al. (2019) and Esplin & Luhman (2019) as red squares. The *Euclid* observation field of view is represented by a white square. (Photograph credit: Bobby White).

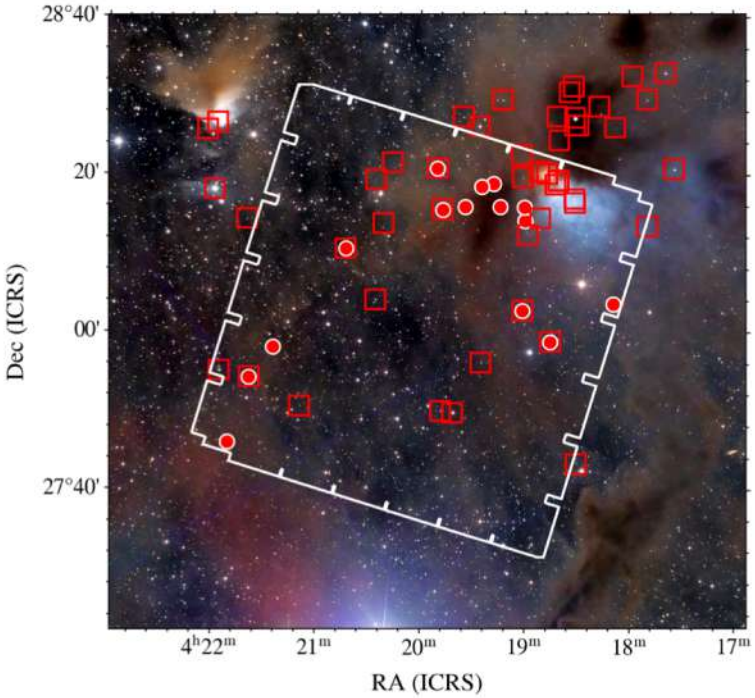
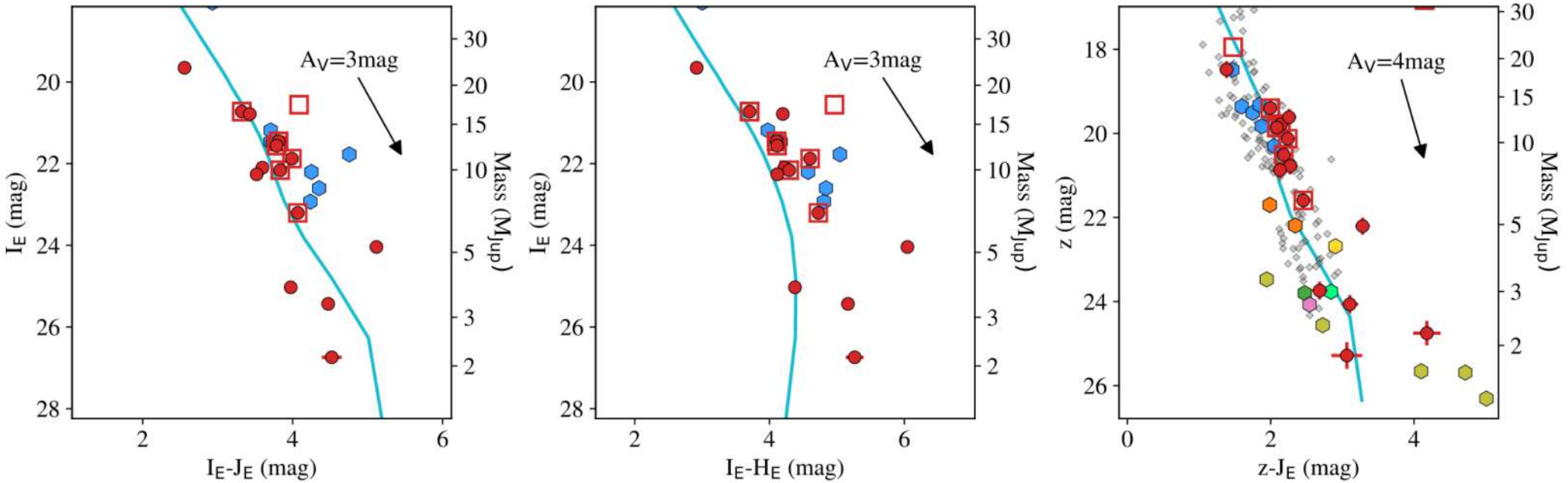


Fig. 7. Spatial distribution of our candidates (red circles) and of known members from Esplin & Luhman (2019) and Galli et al. (2019, red crosses). The *Euclid* VIS image field ofview is represented as a white rectangle. Photograph credit: Chris Fellows.

Bouy, H., et al.: A&A, 696, A80 (2025)



Internal
Astrometric
Precision
Euclid
+/- 2.5 mas

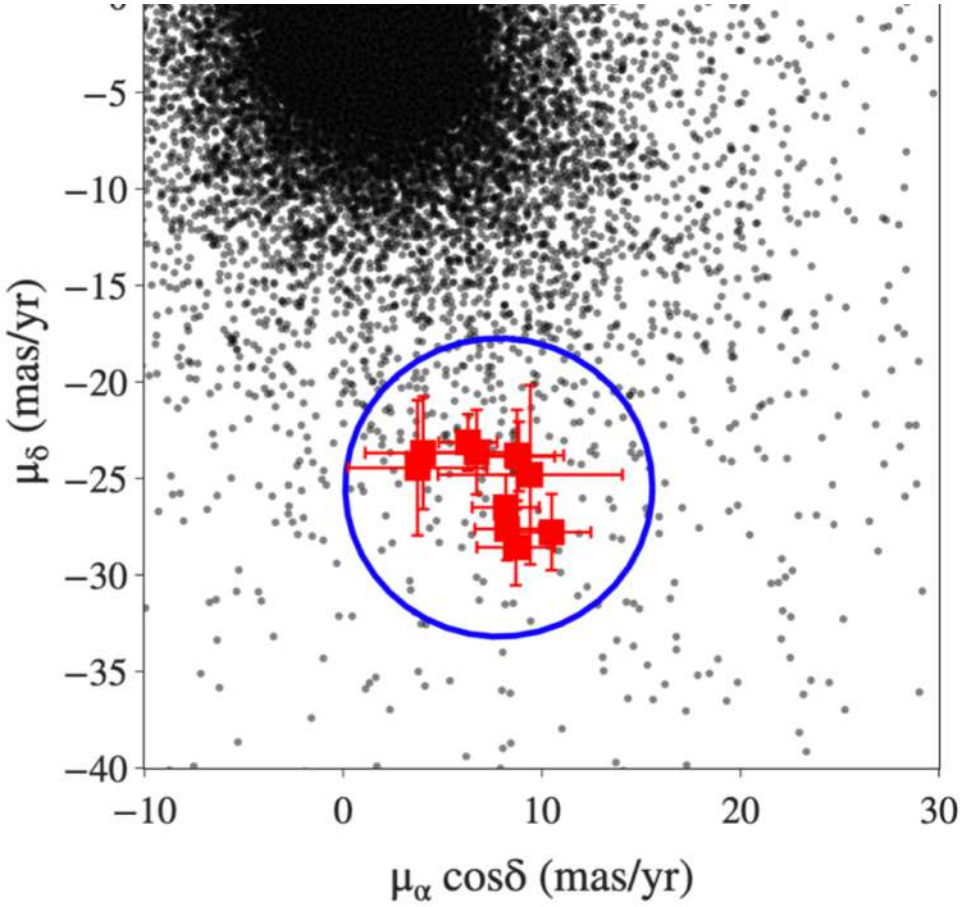


Fig. 4. Proper motion diagram for the sources in our catalog, selected based on their morphology. The members from Galli et al. (2019) and Esplin & Luhman (2019) with a counterpart in our catalog are represented as red squares. A blue circle shows the area we used for the member selection.

What Euclid provides:

Deep optical & NIR imaging

High spatial resolution

Deep low-resolution NIR spectroscopy

Large area coverage

Homogeneous & stable dataset

What Euclid lacks:

Time domain astrometry

Full sky coverage

Euclid – Gaia NIR synergies:

Euclid´s imaging reaches into the planetary domain in nearby SFRs

Photometric selection of candidates is complex

Euclid spectroscopy useful but limited

Membership assessment in the Substellar regime needs Euclid & Gaia NIR combination (NIR parallaxes & proper motions)

Pre-registration Open!!

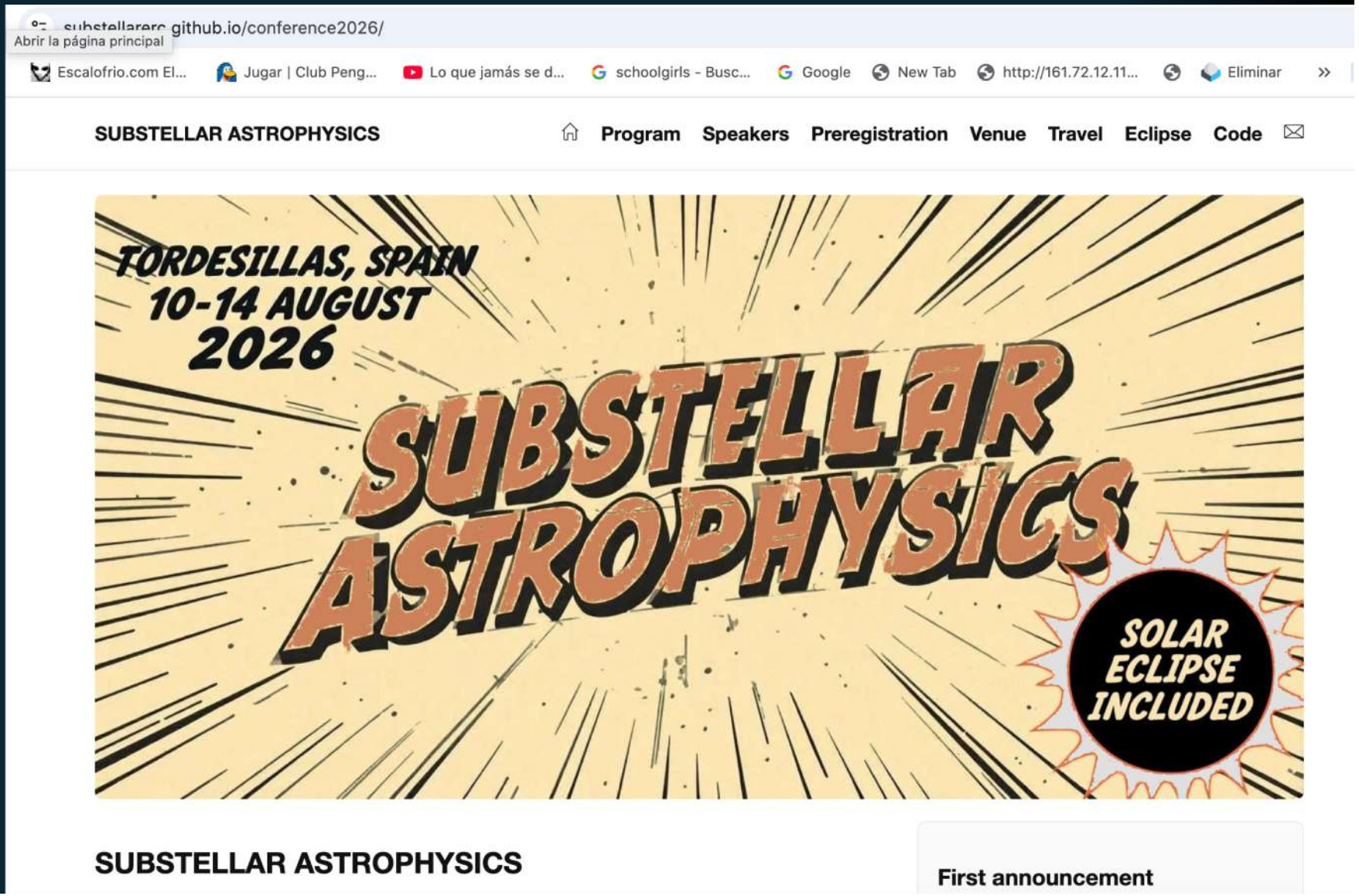
Deadline Feb 15h

Limited capacity (45 rooms)

https://substellarerc.github.io/conference2026/registration.html

substellar@iac.es





Substellar ERC team

Alberto Escobar
Carlos Domínguez-Tagle
Eduardo Martín
Khalid Barkaoui
Nafise Sedighi
Maruska Zerjal
Nikola Vitas
Sara Muñoz Torres
Tsylia Stiliani

Jun-Yan Zhang (now in Canada)

